AFRL-ML-WP-TP-2006-482

GRAIN BOUNDARY CURVATURE IN A MODEL Ni-BASED SUPERALLOY (PREPRINT)

Kai Song and Mark Aindow

JULY 2006

Approved for public release; distribution is unlimited.

STINFO COPY

MATERIALS AND MANUFACTURING DIRECTORATE
AIR FORCE RESEARCH LABORATORY
AIR FORCE MATERIEL COMMAND
WRIGHT-PATTERSON AIR FORCE BASE, OH 45433-7750

REPORT DOCUMENTATION PAGE

Form Approved
OMB No. 0704-0188

1. REPORT DATE *(DD-MM-YY)*	2. REPORT TYPE	3. DATES COVERED *(From - To)*
July 2006	Journal Article Preprint	N/A

4. TITLE AND SUBTITLE
GRAIN BOUNDARY CURVATURE IN A MODEL Ni-BASED SUPERALLOY (PREPRINT)

5a. CONTRACT NUMBER
F33615-00-C-2-5216

5b. GRANT NUMBER

5c. PROGRAM ELEMENT NUMBER
62712E

6. AUTHOR(S)
Kai Song (University of Connecticut)
Mark Aindow (AFRL/MLLM)

5d. PROJECT NUMBER
K720

5e. TASK NUMBER
01

5f. WORK UNIT NUMBER
01

7. PERFORMING ORGANIZATION NAME(S) AND ADDRESS(ES)

University of Connecticut
Institute of Materials Science
Storrs, CT 06269-3136

Metals Branch (AFRL/MLLM)
Metals, Ceramics, and Nondestructive Evaluation Division
Materials and Manufacturing Directorate
Air Force Research Laboratory, Air Force Materiel Command
Wright-Patterson Air Force Base, OH 45433-7750

8. PERFORMING ORGANIZATION REPORT NUMBER

9. SPONSORING/MONITORING AGENCY NAME(S) AND ADDRESS(ES)
Materials and Manufacturing Directorate
Air Force Research Laboratory
Air Force Materiel Command
Wright-Patterson AFB, OH 45433-7750

10. SPONSORING/MONITORING AGENCY ACRONYM(S)
AFRL-ML-WP

11. SPONSORING/MONITORING AGENCY REPORT NUMBER(S)
AFRL-ML-WP-TP-2006-482

12. DISTRIBUTION/AVAILABILITY STATEMENT
Approved for public release; distribution is unlimited.

13. SUPPLEMENTARY NOTES
The U.S. Government is joint author of this work and has the right to use, modify, reproduce, release, perform, display, or disclose the work.

Journal article submitted to Acta Materialia, published by Elsevier B.V.

PAO Case Number: AFRL/WS 06-1882, 09 Aug 2006.

14. ABSTRACT
The local grain boundary curvature in a model Ni-based superalloy was measured experimentally using Dehoff's tangent count method. The results show that, in materials containing significant amounts of second-phase particles, the curvature parameter κ, which relates the mean local curvature to the grain size, can adopt far lower values than have been reported previously. It is also shown that the value of κ is not a constant, as is usually assumed, but instead varies both with the volume fraction of second-phase particles and with the holding time during high-temperature annealing. The lowest values for κ were obtained for high particle volume fractions and long annealing times. Since the local boundary curvature constitutes the driving force for grain growth, these observations could help to explain grain growth phenomena in heavily pinned systems.

15. SUBJECT TERMS
Annealing, Ni alloys, grain size, grain growth, grain boundary curvature

16. SECURITY CLASSIFICATION OF:			17. LIMITATION OF ABSTRACT:	18. NUMBER OF PAGES	19a. NAME OF RESPONSIBLE PERSON (Monitor)
a. REPORT	b. ABSTRACT	c. THIS PAGE			Rollie Dutton
Unclassified	Unclassified	Unclassified	SAR	28	19b. TELEPHONE NUMBER *(Include Area Code)* N/A

Standard Form 298 (Rev. 8-98)
Prescribed by ANSI Std. Z39-18

Text

Grain Boundary Curvature in a Model Ni-Based Superalloy

Kai Song and Mark Aindow*

Institute of Materials Science, University of Connecticut, Storrs, CT 06269-3136, USA

and

Materials Science and Engineering Program, Department of Chemical, Materials and Biomolecular Engineering, University of Connecticut, Storrs, CT 06269-3222, USA

* Author for correspondence, Email: m.aindow@uconn.edu

Abstract

The local grain boundary curvature in a model Ni-based superalloy was measured experimentally using Dehoff's tangent count method. The results show that, in materials containing significant amounts of second-phase particles, the curvature parameter κ, which relates the mean local curvature to the grain size, can adopt far lower values than have been reported previously. It is also shown that the value of κ is not a constant, as is usually assumed, but instead varies both with the volume fraction of second-phase particles and with the holding time during high-temperature annealing. The lowest values for κ were obtained for high particle volume fractions and long annealing times. Since the local boundary curvature constitutes the driving force for grain growth, these observations could help to explain grain growth phenomena in heavily pinned systems.

Key Words: Annealing; Ni alloys; grain size; grain growth; grain boundary curvature

1. Introduction

In studies of grain growth, the grain boundary curvature is an essential parameter because it represents the driving force for grain boundary (GB) migration. The thermodynamic driving force for normal grain growth is usually expressed as:

$$P = 2\gamma_S H \tag{1}$$

where γ_S is the grain boundary surface energy and H is the surface-weighted average of the local curvature over all GBs. Experimentally, the curvature H can be obtained from area tangent and linear intercept measurements [1–3], and is given as:

$$H = \pi T_A I/2 \tag{2}$$

where T_A is the number of points of tangency per unit area between a sweeping test line and a curved grain boundary trace on a 2D cross section, and I is the mean linear intercept. Conventionally, H is often replaced by the linear intercept and is expressed in the following form [4–7]:

$$H = \kappa * I^{-1} \tag{3}$$

The curvature parameter κ is the factor required to describe the driving force for normal grain growth relative to the grain size. Substituting κ into Eq. (1) yields:

$$\mathrm{P} = 2\gamma_\mathrm{S}(\kappa/\mathrm{I}) \tag{4}$$

which is the expression frequently used for modeling grain growth. In most cases, κ is assumed to be a constant specific to the system under consideration [8], with the value of κ depending

upon the topology of the grain structure. Thus, $\kappa = 0$ corresponds to completely flat GBs, while $\kappa = 3/2$ corresponds to spherical grains. For real grain structures, κ adopts intermediate values. For example, Patterson and Liu [5] measured the GB curvature in high-purity aluminum and obtained a value of 0.31 for κ: this corresponds to a driving force for grain growth approximately three times smaller than the value quoted in conventional models.

Considering the importance of curvature in grain growth, however, there have been surprisingly few experimental measurements of H and κ reported. In an early paper, Haroun and Budworth [9] reported curvature measurements from GBs in magnesia, but their measurements involved certain geometrical assumptions. Aside from the work by Patterson and Liu [5], the only other known measurements of H and κ based on the tangent count method are those by Rios and Fonseca [6, 7] for an Al-1 mass% Mn alloy, which contained Al_6Mn particles. These latter authors obtained very similar results to Patterson and Liu, although the numerical values quoted differ by a factor of 2 due to differences in the definition for H.

All of the previous measurements of H and κ have been performed either in pure materials [5, 9] or in dilute alloys [6, 7]: we are not aware of any similar studies on materials containing significant volume fractions of second-phase particles. In our work we have studied grain growth phenomena in powder metallurgy Ni-based superalloys whose initial microstructure consists of a face-centered cubic γ matrix, up to 40% by volume of the $L1_2$ γ' phase, and <1% by volume of inert precipitates (carbides, borides, etc.). During thermal exposure at temperatures above 1100˚C, the γ' phase dissolves into the γ matrix, and this has a profound effect on the grain growth behavior. The grain growth data are reported elsewhere, but in this paper we describe a study of the GB curvature in these superalloy samples. It is shown that the γ' phase can have a profound impact upon the curvature of the boundaries, with far lower values of κ than have been

reported previously. Moreover, the GB curvature is not a constant for such alloys, but instead correlates strongly with the volume fraction of the second phase particles and the heat-treatment holding time.

2. Experimental Materials and Methods

The alloy used in this study was a model powder metallurgy Ni-based superalloy whose composition is Ni - 20.3Co - 14.8Cr - 4.6Al - 3.9Mo - 3.7Ti - 0.08Zr - 0.08C - 0.02B - 0.011Y (all in wt. %): this resembles the chemistry of the matrix phase mixture in the commercial alloy IN100 at the solution heat-treatment temperature (1143 °C). This alloy was produced as part of a program to develop analytical models for the mechanical behavior and microstructural development in alloys such as IN100 [10]; and was chosen for the investigation described here because it contains low levels of impurities, has a highly homogenous microstructure, and has a fine initial grain size.

The alloy was heat-treated at elevated temperatures to study the grain growth behavior. Firstly, small coupons of the alloys, around 2×2×0.2 cm, were cut from the bulk material. The small sample size was chosen so that the sample could be heated or cooled as quickly as possible. The samples were inserted into a pre-heated tube furnace, and held under flowing Ar for times ranging from 2 min to 4800 min to investigate the isothermal grain growth. The heat-treatments were conducted at temperatures between 1093 °C and 1270 °C: since the solvus for the primary γ' phase is around 1143°C [11, 12], we refer to samples heat-treated above and below this temperature as super-solvus and sub-solvus, respectively. At the end of each heat-treatment the sample was removed from the furnace quickly and then water-quenched to minimize any

microstructural changes upon cooling.

The grain structure was characterized using scanning electron microscopy (SEM). The surfaces of the coupons were firstly prepared using standard metallographic grinding and polishing techniques. The GBs were then revealed by immersion-etching the sample in waterless Kalling's solution for a period of 1–3 min, while the γ' particles were defined by etching the sample in Glycerygia for around 20 s [13]. Secondary electron images were obtained from these samples using a JEOL 6335F field-emission SEM operating at an accelerating voltage of 30 kV. The grain size was evaluated by measuring the mean linear intercept (I), and the mean boundary curvature (H) was obtained by using the tangent count method, as given in Eq. (2). The volume fraction of the γ' particles was determined using the point count method.

3. Experimental Results

A general overview of the microstructural development in these samples, with particular emphasis on the grain growth phenomena, is presented elsewhere [12]. In this paper we consider only those aspects directly pertinent to the issue of local boundary curvature.

3.1 Effect of Particle Volume Fraction

For the sub-solvus heat treatment temperatures used in this study, the equilibrium volume fraction of the γ' phase is rather lower than that in the initial microstructure (≈ 40%). As such, partial dissolution of the γ' phase occurs during these heat-treatments. An SEM micrograph of a typical sub-solvus microstructure is shown in Fig. 1: this sample was held at 1127°C for 300 min. The light areas correspond to the lightly etched γ matrix grains, the fine bright lines correspond

to protruding ridges that delineate the γ grain boundaries, the dark areas are deep etch pits corresponding to the positions of the γ' particles, and the small bright particles are the inert precipitates. The volume fraction of the γ' phase, V_f, is 5.8% for this sample and this value tends to 0% as the heat treatment temperature approaches the solvus at 1143˚C. The M_3B_2-type borides and $M_{23}C_6$-type carbides present in the initial microstructure are unstable at the heat-treatment temperatures used in this study and so all of the inert precipitates observed in such images are MC-type carbides [11, 12]. The volume fraction of these MC-type carbides is ≈0.6% in each case.

To show the effects of γ' particle volume fraction on the boundary curvature we consider the data from a series of ten samples held at various temperatures for 300 min. The values of H and I obtained from these samples are plotted in Fig. 2 as a function of the heat-treatment temperature. While the grain size for these samples increases steadily with the heat-treatment temperature the mean curvature exhibits a maximum value at around 1127°C. This is clearly inconsistent with the normal assumption that GB curvature varies inversely with the grain size. The reason for this discrepancy is that the curvature parameter κ is no longer a constant in an alloy that contains a significant volume fraction of second-phase particles. The variation of κ and the volume fraction, V_f, of the γ' particles with heat-treatment temperature for these samples is shown in Fig. 3. For the sample heat-treated at 1093˚C, in which $V_f \approx 23\%$, the value of κ is just 0.064: this is much smaller than any value reported previously. For samples heat-treated at higher temperatures, however, V_f is lower and the values of κ are higher, indicating that it is the particle/GB interactions that reduce the curvature. The value of κ continues to increase with increasing heat-treatment temperature until about 1138˚C where $V_f < 1\%$. For this sample, and indeed for all samples heat-treated at super-solvus temperatures for 300 min, κ adopts a value of

≈ 0.33: this is consistent with the values reported by Patterson and Liu [5], and by Rios and Fonseca [6, 7].

3.2 Effects of Heat-Treatment Time

It was found in this study that κ not only depends on the heat-treatment temperature but also correlates with the holding time. The variation of κ with the holding time for samples heat-treated at five different temperatures is shown in Fig. 4. In each case, the value of κ after 30 min is higher than that after 10 min. This corresponds to the period over which the γ' phase is dissolving and is, therefore, consistent with the effect of particle volume fraction noted in Section 3.1. Thereafter, the samples heat-treated at 1132˚C, 1177˚C and 1216˚C exhibit a stable value of κ from 30 to 300 min, followed by slowly decreasing values from 300 to 4800 min. For the samples heat-treated at 1110˚C and 1127˚C, however, there is no obvious plateau and the decrease in κ from 30 to 4800 min is more pronounced.

The corresponding grain growth data for these samples are presented in Fig. 5, and in each case the grain growth stagnates because of particle pinning effects. It is seen that for the samples heat-treated at 1132˚C, 1177˚C and 1216˚C, it takes around 300 min for the grain growth to stagnate. For the samples heat-treated at 1127°C and 1110°C, grain growth is essentially stagnant after 30 min of heat-treatment. This is because the pinning force at lower temperatures is much higher due to the higher V_f of the γ' phase. By comparing Figs. 4 and 5, it appears that after the initial increase in κ, the value remains stable during grain growth, but decreases once grain growth stagnates.

3.3 Boundary Curvature and Particle Interactions

The data presented in Sections 3.1 and 3.2 indicate that GB/particle interactions can have a profound effect upon the curvature, leading to small values for κ when V_f is high. The effects of the particles were revealed more directly in SEM images such as Figs. 6 and 7, which were obtained from a super-solvus (1177˚C) and a sub-solvus (1110˚C) sample, respectively. In the super-solvus sample ($\kappa \approx 0.33$ and $V_f \approx 0$) many of the GBs are curved, whereas in the sub-solvus sample ($\kappa \approx 0.094$ and $V_f \approx 9.8\%$) the majority of the GBs are straight. Moreover, in the sub-solvus samples there is a strong correlation between the curvature of *individual* boundaries and the presence or otherwise of particles. In Fig. 7 the boundaries that contain particles are rather flat, whereas the particle-free boundaries are more obviously curved. The implication here is that the volume-fraction dependence of κ may arise from the variation in the degree of boundary/particle contact. This was confirmed by measuring the apparent percentage of GBs in contact with the γ' particles ($\%GB_{app}$) from the sub-solvus samples held at various temperatures for 300 min: a plot of these data against V_f is shown in Fig. 8.

4. Discussion

The data presented here show that the curvature parameter κ can adopt much smaller values than have been reported previously, that the value depends upon the volume fraction of the second-phase particles, and that this is related to the degree of GB/particle contact. This is broadly consistent with what one might expect on the basis of previous treatments of GB/particle interactions using computer simulations, theoretical analyses and indirect experimental approaches (e.g. [14-16]). In simulation of 2D grain growth, Srolovitz *et al.* [14] found that the

GB curvature can be eliminated by the particles sitting at boundaries and vertices, but Hillert [15] showed that these effects should be rather different for 2D and 3D grain structures. Doherty *et al.* [16] extended the simulations of GB curvature removal by second-phase particles to 3D grain structures. These latter authors also analyzed the grain size distributions in grain structures with and without second-phase pinning particles, and concluded that in both 2D and 3D grain structure, particles in grain corners and at grain edges can remove the curvature of the GB. These effects are shown clearly in images such as Figure 7 from the sub-solvus samples, wherein the boundaries that contain particles consist of rather flat segments whilst the particle-free boundaries are more obviously curved.

The reasons for the temporal variation of κ, shown in Fig. 4, are less obvious. The increase in κ over the first 30 min is related to the dissolution kinetics for the γ' phase in this alloy at these temperatures. Thus, as V_f falls over this period, κ rises as expected from the data shown in Fig. 3. The equilibrium value for V_f is reached within 30 min, and thereafter κ adopts a constant value during grain growth, as reported previously for pure metals [5] or alloys with stable particles [6,7]. More interestingly, at each of the temperatures considered here the value of κ *decreases* once grain growth stagnates. Moreover, the magnitude of this decrease is somewhat larger for the samples with higher V_f. As far as we are aware, this effect has not been reported previously and the causes are unclear. This effect cannot be due to the coarsening of the pinning particles at the heat-treatment temperature since coarsening would lead to a reduction in the degree of grain boundary contact and would cause an *increase* in the value of κ. One possible explanation is the process of GB rotation described by Srolovitz *et al.* [14]: "Grain boundaries which intersect particles are free to rotate about the particle center. When this is combined with the ability of the vertex to undergo a rotation and limited translation, the curvature on the grain

boundary between the vertex and the particle can readily be eliminated. Curvature eliminated in this fashion may be stored at the particle as a sharp boundary bend". Fig. 9 is a schematic diagram showing this process; and several examples of sharp boundary bends at γ' particles are evident in Figure 7. It is important to recall that the GB must be pinned strongly by the particle for the above mechanism to take operate; otherwise the GB may break away from the particle, rather than rotating around it. We note, however, that grain growth stagnation represents the state in which the unpinning of GBs from the particles becomes negligible. Indeed, it may be for this reason that the value of κ only decreases after grain growth stagnates. Moreover, the larger decreases in κ for the samples with higher V_f are consistent with such a mechanism since the degree of GB/particle contact is higher for these samples.

Based on the above discussion, we would expect the second-phase particles to play two different roles in the inhibition of grain growth for such alloy systems. Firstly, the particles will provide a pinning force that retards the migration of the GBs. Secondly, the particles that lie on GBs will eventually remove the local GB curvature and decrease the overall driving force for grain growth. A consequence of the second role is that, although the pinning particles will coarsen continually in the heat-treatment, the decrease in the pinning force due to particle coarsening might be counteracted by the decrease of the overall driving force, leading to a stable limiting grain size. As an example of this, we note that the sub-solvus sample heat-treated at 1132˚C, for which grain growth stagnation occurs somewhere between 300 and 600 min, the grain size is essentially constant, even after 4800 min when the particles have coarsened significantly [11,12]. Thus, these processes could help to explain the microstructural stability of such strongly pinned alloy systems.

5. Summary

Samples of a model Ni-based superalloy have been subjected to a variety of heat-treatments at temperatures around the γ' solvus, resulting in microstructures with different γ grain sizes and volume fractions of the γ' phase. Measurements of the mean local γ grain boundary curvature, H, have been performed using Dehoff's tangent count method. These data have been used to obtain values for the curvature parameter κ, which relates H to the γ grain size. The main points that have been established are:

1. The value of κ varies with the volume fraction, V_f of the γ' phase. For super-solvus samples, in which $V_f = 0$, $\kappa \approx 0.33$, which is consistent with the values reported for other systems. For sub-solvus samples, however, values of κ as low as 0.064 have been obtained.
2. The value of κ varies with the duration of the heat treatment. Initially, κ increases as the γ' phase dissolves. Once the equilibrium V_f is reached, κ adopts a constant value during grain growth. When the grain growth stagnates at the Zener limiting grain size, however, there is a steady decrease in κ and the magnitude of this depends to some extent on V_f.
3. The degree of γ' particle / γ grain boundary contact is proportional to V_f.

Thus, the V_f dependence of κ is consistent with what one would expect for the removal of local grain boundary curvature by individual γ' particles. However, the reduction in κ after grain growth stagnation, where V_f is constant, requires an alternate mechanism such as the boundary rotation process described by Srolovitz *et al.* This process leads to a reduced driving force for grain growth and may help to explain the stability of the grain structure in such strongly pinned systems, even during subsequent coarsening of the pinning particles.

Acknowledgements

This work was supported by DARPA/USAF under Contract No F33615-00-2-5216 with Dr R. Dutton as technical monitor. The authors would like to thank Dr. Mike Savage of Pratt and Whitney for providing the alloys used in this investigation.

References

[1] DeHoff RT. Trans AIME 1967; 239:617.

[2] Cahn JW. Trans AIME 1967; 239:610.

[3] Dehoff RT. The Geometrical Meaning of the Integral Mean Curvature. In: Microstructural Science, vol. 5. New York (NY): American Elsevier Pub., 1977. p. 331.

[4] Nielsen JP, Stone LP. Grain Boundary Curvature in Annealed Beta Brass. In: Hu H, Ed. The Nature and Behavior of Grain Boundaries. New York (NY): Plenum Press, 1972. p. 229.

[5] Patterson BR, Liu Y. Metall Trans 1992; 23A:2481.

[6] Rios PR, Fonseca GS. Scripta Mater 2004; 50:1373.

[7] Rios PR, Fonseca GS. Scripta Mater 2005; 52:893.

[8] Wörner CH. Scripta Metall 1989; 23:1909.

[9] Haroun NA, Budworth DW. J Mat Sci 1968; 3:326.

[10] Milligan WW, Orth EL, Schirra JJ, Savage MF. Effects of Microstructure on the High Temperature Constitutive Behavior of IN100. In: Green KA et al., Ed. Superalloys 2004: TMS, 2004. p. 331.

[11] Song K, PhD thesis, University of Connecticut, 2005.

[12] Song K and Aindow M, in preparation.

[13] Wusatowska-Sarnek AM, Blackburn MJ, Aindow M. Mater Sci Eng 2003; A360:390.

[14] Srolovitz DJ, Anderson MP, Grest GS, Sahni PS. Acta Metall 1984; 32:1429.

[15] Hillert M. Acta Metall 1988; 36:3177.

[16] Doherty RD, Li K, Anderson MP. Particle Limited Grain Growth: Experiments and Simulations. In: Weiland H, Adams BL, Rollett AD, Ed. Grain Growth in Polycrystalline Materials III: TMS, 1998. p. 271.

Figure Captions

Figure 1: Secondary electron SEM micrograph showing the typical sub-solvus microstructure of a sample heat-treated at 1127˚C for 300 min.

Figure 2: Variation of mean grain γ size, *I,* and mean grain boundary curvature, *H,* with heat-treatment temperature, *T,* in samples heat-treated for 300 min. The error bars for *I* and *H* correspond to the standard errors (σ_M) on these data, and are omitted for *I* where the bars would be smaller than the white squares. Since the values for *H* are obtained using Eq. (2), the σ_M values for *H* were calculated from those for *I* and T_A.

Figure 3: Variation of γ' volume fraction, V_f, and curvature parameter, κ, with heat-treatment temperature, *T,* in samples heat-treated for 300 min. Error bars for V_f correspond to the standard deviation (σ) of these data, and are omitted where the bars are smaller than the black squares.

Figure 4: Variation of curvature parameter, κ, with the heat-treatment time, *t*, for samples heat-treated at five different temperatures.

Figure 5: Variation of the mean γ grain size, *I*, with heat-treatment time, *t*, for samples heat-treated at five different temperatures. Error bars are omitted for clarity, but the values of σ_M on these data are 0.28-0.32, 0.35-0.43, 0.42-0.76, 0.92-1.09 and 0.89-1.13 μm for 1100, 1127, 1132, 1177 and 1216˚C, respectively.

Figure 6: Secondary electron SEM micrograph showing the typical super-solvus microstructure

of a sample heat-treated at 1177˚C for 300 min. The white arrows indicate examples of curved GBs.

Figure 7: Secondary electron SEM micrograph showing the sub-solvus microstructure of a sample heat-treated at 1110˚C for 300 min. The white arrows indicate examples of curved particle-free GBs, whereas the black arrows indicate examples of flatter GBs that contain γ' particles: in several cases there is a sharp change in boundary orientation at these particles.

Figure 8: Variation of the apparent percentage of pinned grain boundaries, $\%GB_{app}$, with γ' volume fraction, V_f, in samples heat-treated for 300 min. The error bars for both V_f and $\%GB_{app}$ correspond to the standard deviation (σ) of these data, and are omitted where the bars would be smaller than the black squares.

Figure 9: Schematic diagram showing the boundary rotation mechanism for the removal of GB curvature (following Srolovitz [14]). The black arrow indicates the initial configuration of the curved GBs and the white arrow indicates the GB configuration after the boundary rotation.

Figure(s)

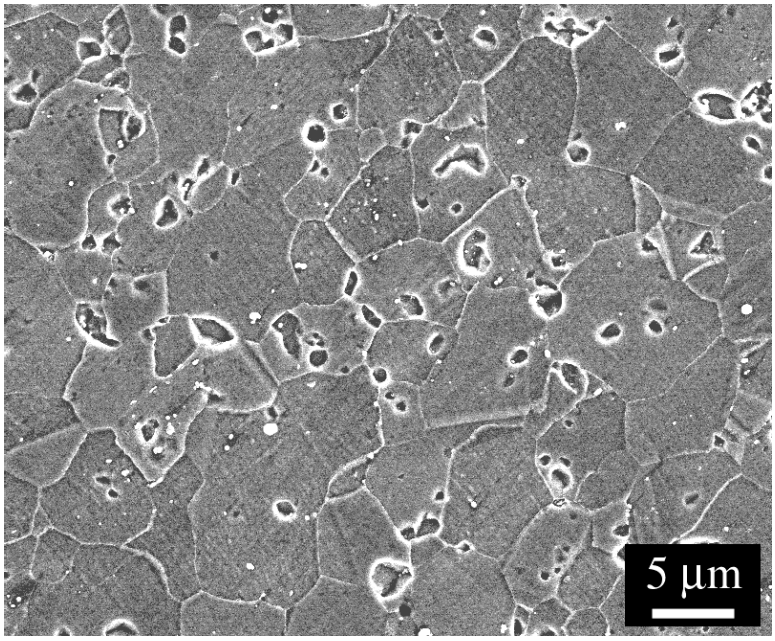

Figure 1

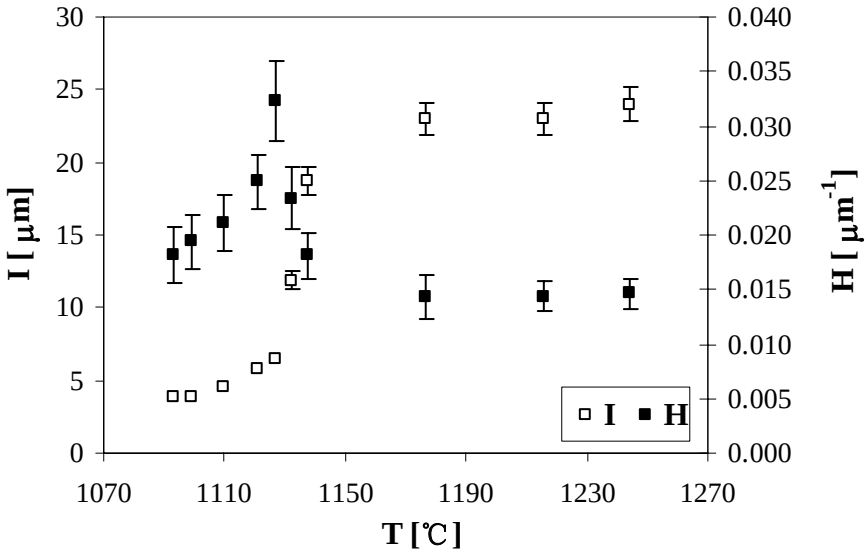

Figure 2

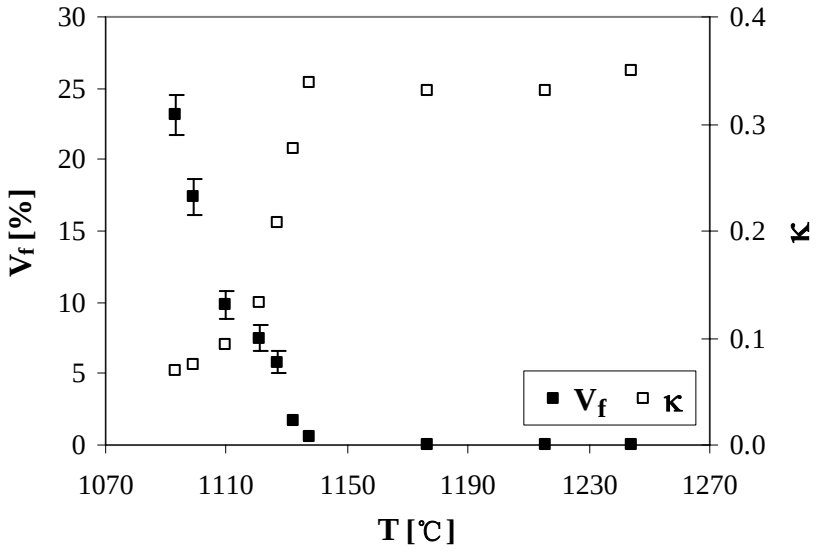

Figure 3

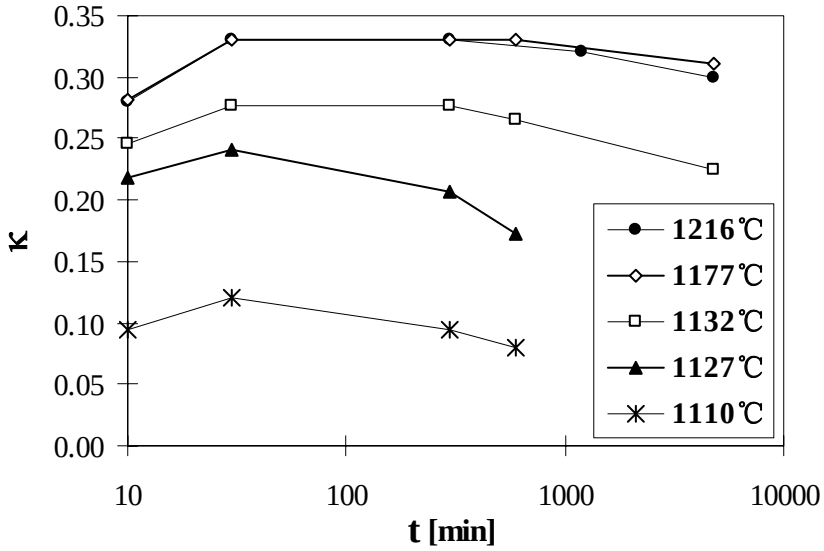

Figure 4

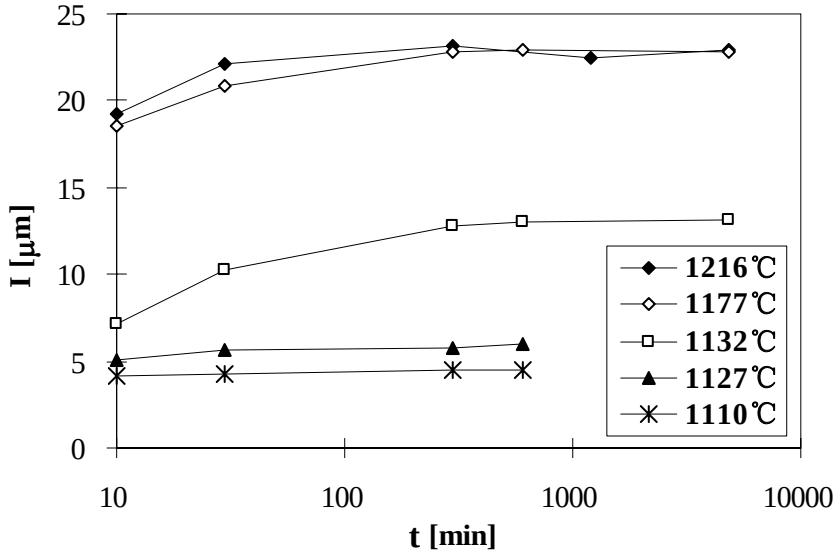

Figure 5

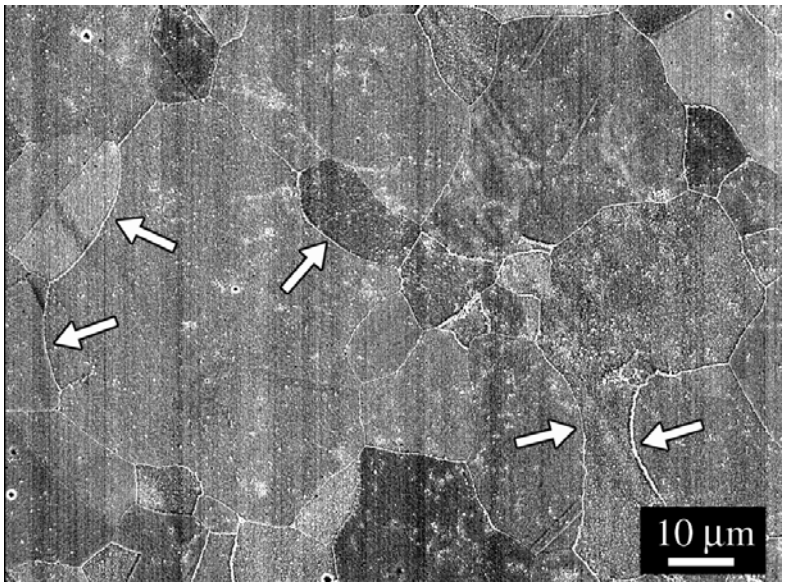

Figure 6

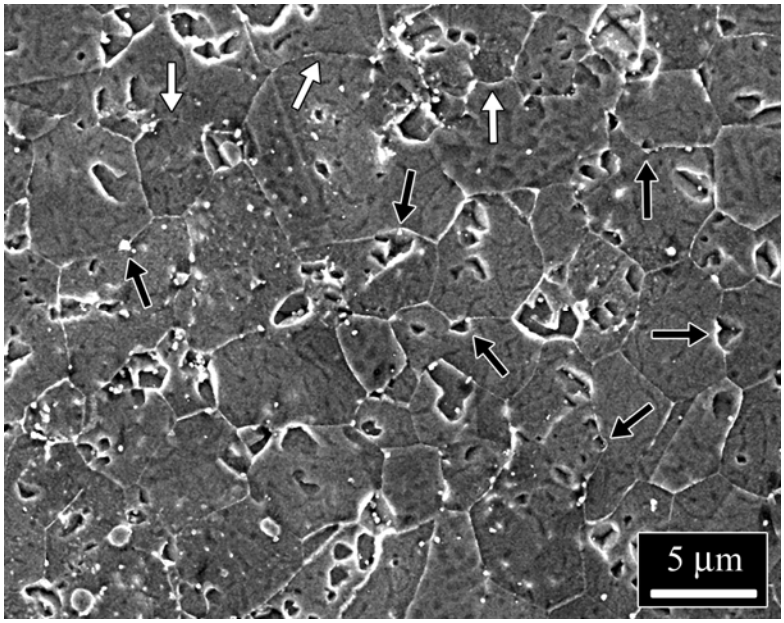

Figure 7

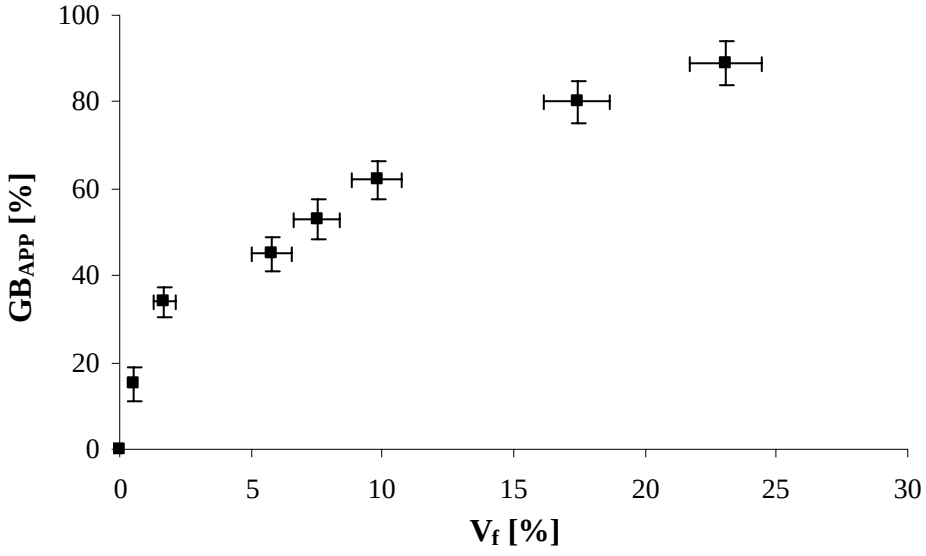

Figure 8

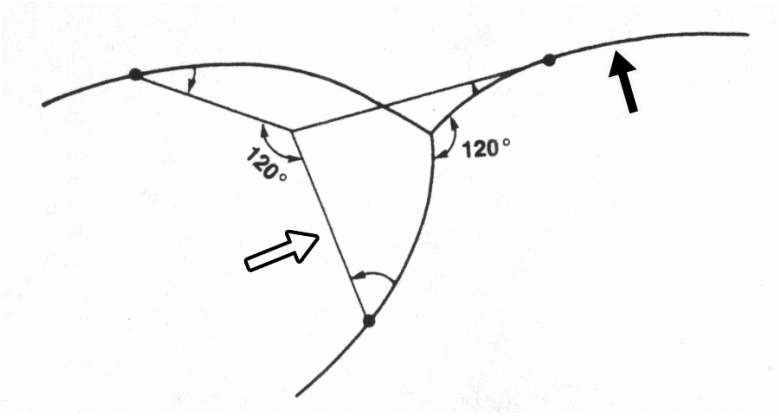

Figure 9